

# Experimental Verification of the Roles of Intrinsic Matrix Viscoelasticity and Tension-Compression Nonlinearity in the Biphasic Response of Cartilage

Chun-Yuh Huang  
Michael A. Soltz  
Monika Kopacz  
Van C. Mow  
Gerard A. Ateshian<sup>1</sup>

Departments of Mechanical Engineering and  
Biomedical Engineering,  
Columbia University,  
500 West 120th St.,  
New York, NY 10027

*A biphasic-CLE-QLV model proposed in our recent study [2001, J. Biomech. Eng., 123, pp. 410–417] extended the biphasic theory of Mow et al. [1980, J. Biomech. Eng., 102, pp. 73–84] to include both tension-compression nonlinearity and intrinsic viscoelasticity of the cartilage solid matrix by incorporating it with the conewise linear elasticity (CLE) model [1995, J. Elasticity, 37, pp. 1–38] and the quasi-linear viscoelasticity (QLV) model [Biomechanics: Its foundations and objectives, Prentice Hall, Englewood Cliffs, 1972]. This model demonstrates that a simultaneous prediction of compression and tension experiments of articular cartilage, under stress-relaxation and dynamic loading, can be achieved when properly taking into account both flow-dependent and flow-independent viscoelastic effects, as well as tension-compression nonlinearity. The objective of this study is to directly test this biphasic-CLE-QLV model against experimental data from unconfined compression stress-relaxation tests at slow and fast strain rates as well as dynamic loading. Twelve full-thickness cartilage cylindrical plugs were harvested from six bovine glenohumeral joints and multiple confined and unconfined compression stress-relaxation tests were performed on each specimen. The material properties of specimens were determined by curve-fitting the experimental results from the confined and unconfined compression stress relaxation tests. The findings of this study demonstrate that the biphasic-CLE-QLV model is able to describe the strain-rate-dependent mechanical behaviors of articular cartilage in unconfined compression as attested by good agreements between experimental and theoretical curvefits ( $r^2=0.966\pm 0.032$  for testing at slow strain rate;  $r^2=0.998\pm 0.002$  for testing at fast strain rate) and predictions of the dynamic response ( $r^2=0.91\pm 0.06$ ). This experimental study also provides supporting evidence for the hypothesis that both tension-compression nonlinearity and intrinsic viscoelasticity of the solid matrix of cartilage are necessary for modeling the transient and equilibrium responses of this tissue in tension and compression. Furthermore, the biphasic-CLE-QLV model can produce better predictions of the dynamic modulus of cartilage in unconfined dynamic compression than the biphasic-CLE and biphasic poroviscoelastic models, indicating that intrinsic viscoelasticity and tension-compression nonlinearity of articular cartilage may play important roles in the load-support mechanism of cartilage under physiologic loading. [DOI: 10.1115/1.1531656]*

## Introduction

Connective tissues such as articular cartilage exhibit markedly different material properties in tension and compression. This tension-compression nonlinearity in the tissue response is dictated by the collagen content and its microstructural architecture, which govern primarily the tissue's tensile properties, and the proteoglycan content and its molecular organization as well as water content, which govern its compressive properties. In recent studies [1,2], it has been shown that the incorporation of tension-compression nonlinearity in biphasic [3] constitutive models of articular cartilage can considerably improve the prediction of the tissue's response to unconfined compression. The incorporation of intrinsic viscoelasticity of the solid matrix of biphasic cartilage [4]

has also been shown to improve the prediction of experimental response in unconfined compression [5], raising the question as to which of these models is more comprehensive for describing a variety of articular cartilage mechanical behavior.

Many constitutive models of articular cartilage have captured one or more of the observed experimental responses of articular cartilage to various testing modalities. The most commonly employed constitutive models of cartilage include the linear isotropic biphasic theory of Mow et al. [3] and its extensions to nonlinear permeability [6], finite deformation [7,8], and transverse isotropy [9]; the biphasic poroviscoelastic theory of Mak [4] which combines the linear biphasic theory with the quasi-linear viscoelasticity theory of Fung [10]; the electromechanical theory of Frank and Grodzinsky [11] which incorporates electrokinetic effects in the modeling of the mechanical behavior of cartilage; and the triphasic and multiphasic theories [12–14] which account for the flow of ions as well as mechano-electrochemical effects. Recently, new models have also been proposed for cartilage which account for the tension-compression nonlinearity within the context of a poroelastic [1] or biphasic [2] model. Other models have focused on the microstructural response of the tissue [15–17].

<sup>1</sup>Corresponding Author Gerard A. Ateshian, Associate Professor, Columbia University, Department of Mechanical Engineering, 500 West 120th Street, MC 4703, New York, NY 10027 Phone: 212-854-8602 Fax: 212-854-3304 e-mail: ateshian@columbia.edu

Contributed by the Bioengineering Division for publication in the JOURNAL OF BIOMECHANICAL ENGINEERING. Manuscript received Jun. 2001; revised manuscript received Jun. 2002. Associate Editor: M. S. Sacks.

Previous studies have verified some of these models against experiments under different loading configurations including: (1) confined compression creep, stress-relaxation, and dynamic loading of a cylindrical plug of articular cartilage using linear and nonlinear biphasic [3,6,7,18–21], electromechanical [11], and biphasic poroviscoelastic models [22,32]; (2) unconfined compression stress-relaxation and dynamic loading of a cylindrical plug using isotropic [23,24] and transversely isotropic biphasic [9,21], electromechanical [25], biphasic poroviscoelastic [5], and tension-compression nonlinearity models [1,2,26]; (3) indentation of articular layers on their bony substrate using a flat or spherical indenter, using the linear isotropic biphasic [27–30], the linear transversely isotropic biphasic [9,31], and the biphasic poroviscoelastic [32] theories; and (4) uniaxial tensile tests which employ the quasi-linear viscoelasticity theory [33].

Despite the success of these constitutive models in predicting the experimental response of articular cartilage in certain testing configurations, no single constitutive law has successfully described the transient and equilibrium uniaxial tensile and compressive responses of cartilage simultaneously. In our recent study [34], it was demonstrated from a theoretical analysis that a constitutive model which could achieve this goal had to combine the features of several of the previously proposed models in the literature. In particular, it was demonstrated that the biphasic theory of Mow et al. [3] could be extended to incorporate both tension-compression nonlinearity as well as intrinsic viscoelasticity of the solid matrix of cartilage. The biphasic-conewise linear elasticity (CLE) model was proposed by Soltz and Ateshian [2] to account for tension-compression nonlinearity of cartilage based on the bimodular stress-strain CLE constitutive law introduced by Curnier et al. [35]. The biphasic poroviscoelastic model of Mak [4] employs the quasi-linear viscoelasticity (QLV) model of Fung [10] to describe intrinsic viscoelasticity of the solid matrix of cartilage. Both models were combined in a single constitutive model to analyze the response of cartilage to standard testing configurations. Results were compared to experimental data from the literature and it was found that a simultaneous prediction of compression and tension experiments of articular cartilage, under stress-relaxation and dynamic loading, can be achieved when properly taking into account both flow-dependent and flow-independent viscoelastic effects, as well as tension-compression nonlinearity. The objective of the current study is to directly test this biphasic-CLE-QLV model against experimental data from unconfined compression tests under stress-relaxation at slow and fast strain rates, as well as dynamic loading. The hypothesis is that experimental measurements from these tests can be simultaneously modeled only if the tension-compression nonlinearity and the intrinsic matrix viscoelasticity are (both) incorporated into the biphasic theory.

## Materials and Methods

**Experiments.** Twelve full-thickness cartilage cylindrical plugs (diameter=4.78 mm) were harvested from six old bovine glenohumeral joints (6–10 months old) and stored in physiological buffered saline (PBS) solution at  $-20^{\circ}\text{C}$  until the day of testing. Multiple confined and unconfined compression stress-relaxation tests were performed on each specimen, on two consecutive days, as outlined next. On the first day of testing, the specimen was thawed then microtomed by  $\sim 200$  microns in the deep zone to remove subchondral bone. The specimen thickness was then measured using a micrometer device sensing the electrical conductivity of the cartilage ( $h=1.04\pm 0.15$  mm). All compression tests of cartilage plugs were conducted on a custom loading device described previously [2], which consists of a computer-controlled stepper micrometer (Model 18515, Oriol Instruments, Stratford, CT) driving a loading platen or porous indenter, a linear variable differential transformer (LVDT) for measuring specimen deformation (HR 100, Schaevitz Sensors, Hampton, VA), a load cell for monitoring the load response (Sensotec, model 31, Co-

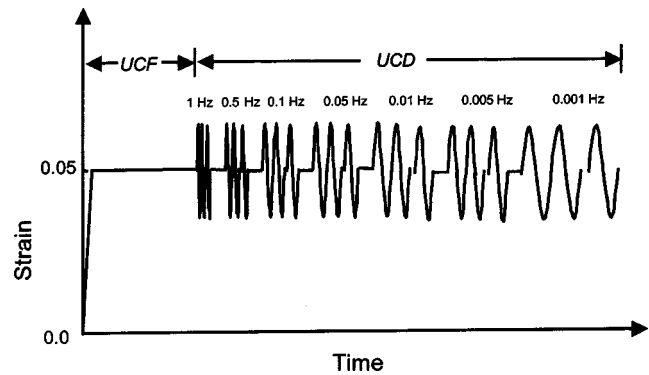


**Fig. 1** Schematic of the testing protocol of the *UCF* and *UCD* tests

lumbus, OH), and testing chambers for confined and unconfined compression, affixed on a two-axis translation stage for alignment. All tests were performed with the chamber filled with PBS solution. For the confined compression tests, the specimen was fit into a confining chamber (4.78 mm diameter) and loaded using a porous-permeable loading platen (4.76 mm diameter, 50% porosity, 45–53  $\mu\text{m}$  pore size). For the unconfined compression tests, the specimen was compressed between two impermeable flat-smooth platens. For each experiment, after mounting the specimen, a tare load of 0.89 N was first applied on the specimen and maintained (using load control via a feedback control algorithm) until equilibrium was achieved ( $\sim 3,000$  s). The criterion for determining equilibrium was that the change in load or displacement falls below the resolution of the load cell (0.02 N) or the LVDT (1  $\mu\text{m}$ ) over a period of at least 300 sec. On day one of testing, following tare loading, a confined compression stress-relaxation test (*CCS*) was performed by applying 5% strain on the specimen at a constant strain rate of  $1.25 \times 10^{-4} \text{ sec}^{-1}$ , then holding the strain at that level until an equilibrium load response was achieved ( $\sim 5,000$  s). Afterward the specimen was unloaded and allowed to recover in PBS solution for an hour; following another tare load application, an unconfined compression stress-relaxation test was also performed, using the same applied strain rate and equilibrium strain magnitude (*UCS*). On the other testing day, following tare loading, an unconfined compression stress-relaxation test was performed with an applied equilibrium strain of 5%, at a fast ramp displacement rate of 1 mm/s (averaging a strain rate of  $\sim 0.96 \text{ sec}^{-1}$ ) (*UCF*); for six of the specimens, without unloading the tissue, the *UCF* test was followed by seven consecutive dynamic unconfined compression tests (*UCD*) with a sinusoidal displacement amplitude of 8  $\mu\text{m}$  and frequencies of 1, 0.5, and 0.1 Hz (10 cycles each), and 0.05, 0.01, 0.005, and 0.001 Hz (5 cycles each). Between consecutive *UCD* tests, the specimen was allowed to recover until the load returned to its value at the start of the first *UCD* test. The testing protocol of the *UCF* and *UCD* tests is shown in Fig. 1. For all load-control (tare loading) and displacement-control (*CCS*, *UCS*, *UCF*, *UCD*) tests, the stepper micrometer was driven by a program created using the LabView data acquisition and control software (National Instruments, Austin, TX). The order of testing (*CCS*+*UCS* versus *UCF* + *UCD*) was randomized over the two consecutive days. Similarly, the order of *CCS* and *UCS* tests was randomized over specimens; however the order of *UCF* and *UCD* tests was not changed since the *UCD* test started from the equilibrium state of the *UCF* test in order to prevent lift-off of the loading platen. After finishing the tests of day one, specimens were allowed to recover in PBS solution for an hour and then frozen at  $-20^{\circ}\text{C}$  overnight. Pilot tests demonstrated that there was no significant adverse effect in cartilage mechanical response between unconfined compression tests performed on the same specimen before and after freezing overnight at  $-20^{\circ}\text{C}$ . Though biochemical degradation

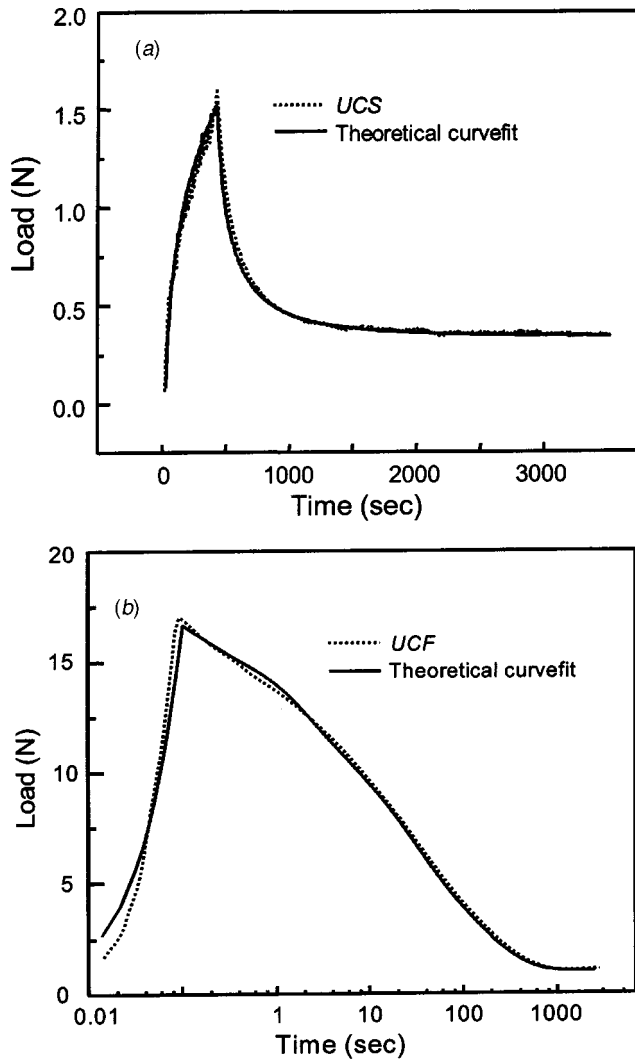


**Fig. 2 Typical experimental responses and theoretical curvefits of the biphasic-CLE-QLV model for unconfined compression stress-relaxation with (a) slow (UCS), and (b) fast (UCF) strain rates**

was not assessed in this study, it was assumed that any potential matrix degradation had a reasonably negligible impact on the measured biomechanical responses.

**Apparatus Compliance.** The fast strain rate experiments and the dynamic experiments (UCF and UCD) typically produced peak reaction forces on the order of 15 N (Fig. 2b). To account for apparatus compliance at these loads, load-deformation curves were obtained in the absence of a cartilage specimen, i.e., with opposing loading surfaces in direct contact. A linear apparatus compliance curve was observed ( $r^2=0.999$ ), with a slope of  $\alpha = 1.1 \mu\text{m/N}$ . This compliance curve was used to correct the experimentally measured specimen deformation for UCF and UCD, by subtracting the apparatus compliance deformation from the total LVDT measurement. All subsequent data analyses were performed on the compliance-adjusted specimen data.

**Data Analysis.** For unconfined compression, the closed-form solution for the biphasic-CLE-QLV model has been described in our recent study [34] and is summarized in Appendix A. The governing equations of the biphasic-CLE-QLV model represent a combination of the biphasic equations of Mow et al. [3], the quasi-linear viscoelasticity theory of Fung [4,10] and the octant-wise orthotropic conewise linear elasticity model of Curnier et al.

[2,35]. In the current implementation of this model, it is assumed that the material exhibits cubic symmetry, that the intrinsic viscoelasticity is the same in bulk and shear deformation as well as in tension and compression [4], and that the tissue properties are homogeneous. The material parameters for this model are  $H_{-A}$ ,  $H_{+A}$ ,  $\lambda_2$ ,  $\mu$ ,  $k_r$ ,  $k_z$ ,  $c$ ,  $\tau_1$ ,  $\tau_2$ ;  $H_{-A}$  is the equilibrium confined compression modulus of the tissue (the “aggregate” modulus) and  $H_{+A}$  is the equivalent modulus in tension;  $\lambda_2$  is the “off-diagonal” modulus which could be determined from the equilibrium ratio of radial stress to axial strain in confined compression (the radial stress being measurable on the side wall, e.g., see the experiments of Khalsa and Eisenberg [36]);  $\mu$  is the equilibrium shear modulus;  $k_r$  and  $k_z$  are the constant tissue permeabilities in the radial and axial directions, respectively;  $[1/\tau_2, 1/\tau_1]$  represents the frequency range over which most of the intrinsic solid matrix viscoelastic energy dissipation occurs under dynamic loading; and  $c$  is a dimensionless constant with  $(1 + c \ln \tau_2/\tau_1)$  representing the factor by which the instantaneous modulus under sudden loading in unconfined compression or uniaxial tension is increased above the value it would assume in the absence of intrinsic solid matrix viscoelasticity. The elastic constants  $H_{-A}$ ,  $H_{+A}$ ,  $\lambda_2$  can be rearranged to provide an alternative set of familiar material parameters: the equilibrium unconfined compression (Young’s) modulus,  $E_{-y}$ ; the equilibrium unconfined compression Poisson ratio  $\nu_{-}$ ; and the equilibrium uniaxial tensile modulus,  $E_{+y}$  [2]. The special case of the biphasic-CLE model can be achieved by letting  $c=0$ , whereas the special case of the biphasic poroviscoelastic model can be obtained by letting  $H_{+A}=H_{-A}\equiv H_A$  and  $\lambda_2=H_A - 2\mu$ .

From the outset, it was recognized that the shear modulus does not independently regulate the response of the tissue to confined and unconfined compression, thus it could not be extracted from these experiments (it is also readily obtainable from torsional shear experiments [2]); hence, eight physically well defined and measurable material constants were sought in the current study. The confined compression aggregate modulus,  $H_{-A}$ , was obtained directly from the equilibrium response of the confined compression stress-relaxation experiment (CCS). The remaining six parameters were obtained from the slow and fast strain rate unconfined compression stress-relaxation experiments (UCS and UCF) as follows. Given,  $H_{-A}$ , initial estimates of  $H_{+A}$ ,  $\lambda_2$ , and  $k_r$  were first obtained by curve-fitting the experimental load response of the UCS test to the biphasic-CLE-QLV equations for unconfined compression stress-relaxation [see Eq. (A1) in Appendix A] with  $c=0$  (no intrinsic viscoelasticity effect), in the time domain. Curve-fitting was performed with the quasi-Newton optimization method for minimizing a function with simple bounds using a finite-difference gradient (IMSL Fortran Numerical Libraries, Visual Numerics, Houston, TX), with the objective function given by the root-mean-square of the residual error between the experimentally measured and theoretically predicted load response,

$$\begin{aligned}
 UCS_{obj} &= \sqrt{\sum_i \{ [F_{theory}(t_i) - F_{experiment}(t_i)] / H_{-A} \varepsilon_0 \pi r_0^2 \}^2 / n_{UCS}} \\
 & \quad (1)
 \end{aligned}$$

where the summation was taken over all time steps,  $n_{UCS}$ . Next, given  $H_{-A}$  and these estimates of  $H_{+A}$ ,  $\lambda_2$ , and  $k_r$ , initial estimates of  $c$ ,  $\tau_1$  and  $\tau_2$  were obtained by curve-fitting the dynamic modulus derived from the experimental response of the UCF test [see Eq. (B5) in Appendix B] to the theoretical modulus predicted by the biphasic-CLE-QLV theory [the ratio of  $\bar{F}(s)/\pi r_0^2$  and  $\bar{\varepsilon}(s)$  in Eq. (A1)]. This curve-fitting was performed in the frequency domain, with the objective function given by

$$UCF_{obj} = \sqrt{\sum_i \{ \text{Re}[G_{theory}(j\omega_i) - G_{experiment}(j\omega_i)]/H_{-A} \}^2 + \{ \text{Im}[G_{theory}(j\omega_i) - G_{experiment}(j\omega_i)]/H_{-A} \}^2 / n_{UCF}} \quad (2)$$

The summation was taken over  $n_{UCF} = 500$  values of  $\omega_i$  sampled uniformly on a base-10 logarithmic scale, with  $\omega_i/2\pi$  ranging from  $10^{-3}$  Hz to 3 Hz. Then, the values of  $H_{+A}$ ,  $\lambda_2$ ,  $k_r$ ,  $c$ ,  $\tau_1$  and  $\tau_2$  were refined by simultaneously curve-fitting the experimental responses of the *UCS* and *UCF* tests to the biphasic-CLE-QLV model, with the objective function given by the sum of  $UCS_{obj}$  and  $UCF_{obj}$  in Eqs. (1) and (2), respectively. Given  $H_{-A}$ ,  $c$ ,  $\tau_1$  and  $\tau_2$ , the constant tissue permeability in the axial direction,  $k_z$ , was determined by curve-fitting the transient response of the *CCS* test using the formulation reported in the study of Mak [4].

The amplitude and phase angle of the dynamic stiffness were determined from the experimental results of the *UCD* tests using the discrete Fourier transform (DFT). These results were used to verify that the transformation from the time domain to the frequency domain performed on the data from the *UCF* test was consistent with the *UCD* results, by comparing the experimental dynamic modulus from the *UCD* tests against the dynamic modulus obtained from the *UCF* test as described in Appendix B. For all tests, the quality of curve-fitting or predictions was assessed using the coefficient of determination  $r^2$  [37]:

$$r^2 = 1 - \frac{\sum (y - y_t)^2}{\sum (y - \bar{y})^2} \quad (3)$$

where  $y$  and  $y_t$  represent the experimental and theoretical variables, respectively, and  $\bar{y}$  is the mean value of  $y$ .

Finally, the curve-fitting process described above was repeated for the case of the biphasic-CLE model and the biphasic poroviscoelastic model as well, to determine the extent to which each of these subset theories could predict the experimental responses.

## Results

The conversion of *UCF* data from the time domain to the frequency domain is shown in Fig. 3 for a typical specimen. In the frequency domain plot, the experimental data from the *UCD* test is also presented in the same figure; the coefficient of determination between the two data sets was found to be  $r^2 = 0.955 \pm 0.037$  over six samples, confirming that good agreement was found between the time domain and frequency domain responses irrespective of the choice of a constitutive model. This result justifies the use of the frequency domain response of the *UCF* test for the curve-fitting of material properties and suggests that the viscoelasticity of cartilage is nearly linear, in the range of compressive strains employed in this study.

Representative theoretical curve-fits and experimental results of the *UCS* and *UCF* tests are presented in Fig. 2 for the biphasic-CLE-QLV theory and in Fig. 4 for the BPVE model. A representative curve-fit of the experimental *CCS* response is also presented in Fig. 5 for the biphasic-CLE-QLV model. Given  $H_{-A}$ ,  $c$ ,  $\tau_1$  and  $\tau_2$ , all curve-fits of the *CCS* using the BPVE model for the determination of  $k_z$  failed to converge, despite increasing the upper bound limit on  $k_z$  to unrealistically high values. Mean and standard deviation of all material properties obtained from curve-fitting of the experimental results of the confined and unconfined compression tests are summarized in Table 1 for each of the three constitutive models (biphasic-CLE-QLV, biphasic-CLE, and BPVE). In addition, for consistency with our earlier study [2], biphasic-CLE properties derived from the *UCS* and *CCS* tests only are also presented in Table 1. According to a Student's pairwise, two-tailed *t*-test analysis ( $\alpha = 0.05$ ), there were no differ-

ences in the elastic and permeability properties between the biphasic-CLE-QLV and the biphasic-CLE (*UCS* and *CCS* tests only) models, with  $p = 0.068$  for  $H_{+A}$ ,  $p = 0.26$  for  $\lambda_2$ ,  $p = 0.54$  for  $k_r$ , and  $p = 0.25$  for  $k_z$ . For the biphasic-CLE-QLV and the biphasic-CLE models, a paired *t*-test analysis found that  $H_{+A} > H_{-A}$  ( $p < 0.0001$ ), confirming tension-compression nonlinearity.

Nonlinear coefficients of determination  $r^2$  for the curve-fits of experimental data are given in Table 2 for each of the constitutive models. A one-way analysis of variance with repeated measures, at a confidence level of  $\alpha = 0.05$ , found a significant difference among the coefficients of determination of the three constitutive models, for both the *UCS* ( $p < 0.0001$ ) and *UCF* ( $p = 0.001$ ) tests. Using a Student-Newman-Keuls post-hoc test on the means, it was found that all three constitutive models differed from one another, with the highest coefficients of determination observed in the biphasic-CLE-QLV theory, followed by the BPVE and then the biphasic-CLE theory, for *UCS* and *UCF*. Since the BPVE

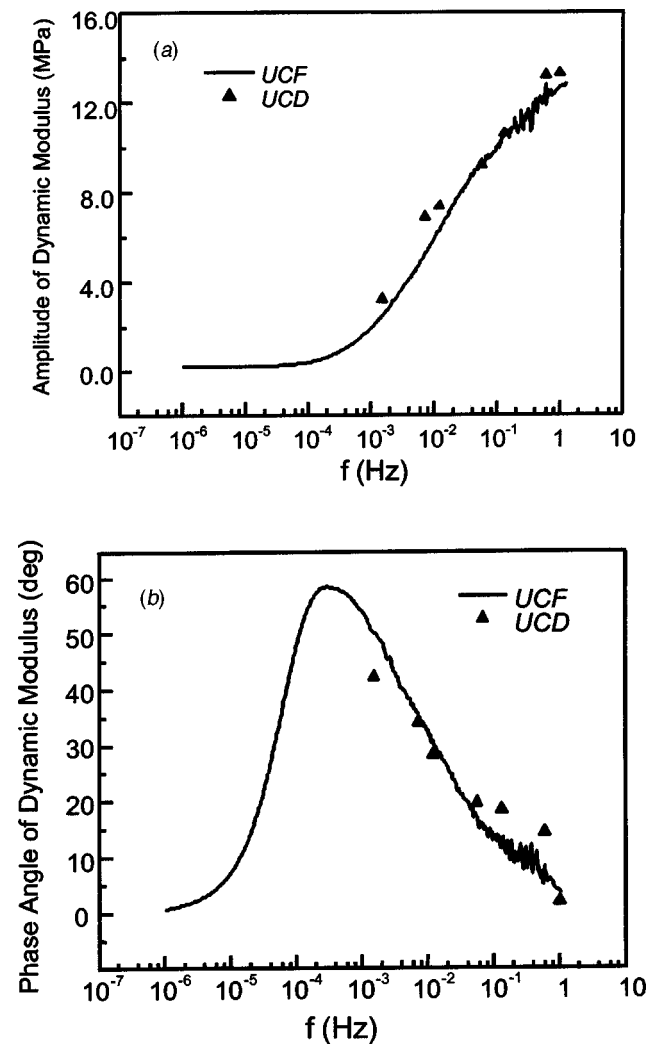
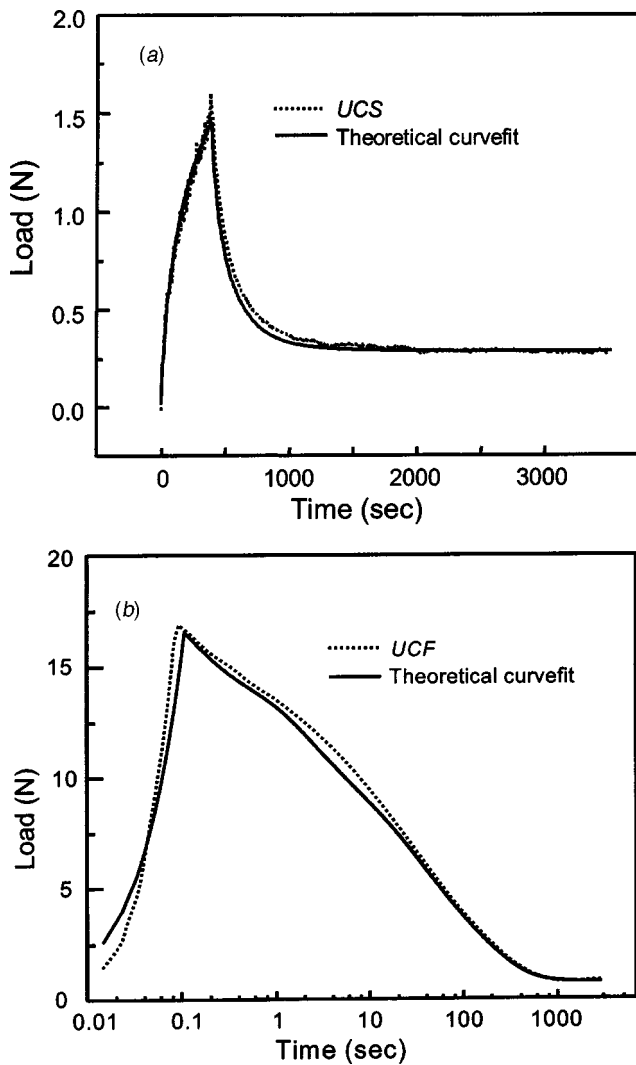


Fig. 3 Conversion of the *UCF* experimental data from the time domain to the frequency domain, using the procedure outlined in Appendix B. The corresponding *UCD* experimental data is also presented for the same typical specimen: (a) amplitude and (b) phase angle of the dynamic modulus.



**Fig. 4 Typical experimental responses and theoretical curve-fits of the BPVE model for unconfined compression stress-relaxation with (a) slow (UCS), and (b) fast (UCF) strain rates**

model could not fit the response of the CCS test,  $k_2$  and  $r^2$  for the BPVE model are not reported in Tables 1 and 2, respectively.

Given all the material properties curve-fitted from the CCS, UCS, and UCF experiments, it was possible to predict the UCD experimental response by substituting these material properties into the theory. Average results for the dynamic modulus (amplitude and phase angle), obtained from the UCD tests on a subset of six specimens, are presented in Fig. 6, together with the theoretical prediction from the biphasic-CLE-QLV model using the mean values of the material properties evaluated over the corresponding six specimens. The agreement between the experimental data and the theoretical prediction, as assessed from the coefficient of determination, was  $r^2 = 0.91 \pm 0.06$ .

## Discussion

Prior to discussing differences among the various constitutive models of cartilage employed in this study, the first observation to be made relates to the validity of using the transient-to-harmonic transformation of the stress-relaxation response employed for the purpose of curve-fitting the UCF data. Buschmann [38] proposed using this type of transformation but cautioned that it is valid only for material responses governed by linear differential equations, since linearity is assumed in the use of the Laplace transformation

from the time to the frequency domain. The typical result presented in Fig. 3 and the high  $r^2$  value reported above between the UCD results and the UCF results transformed into the frequency domain suggest that the transformation is valid for these experiments. There are two practical reasons for using this transformation (as opposed to curve-fitting the UCF response in the time domain, as is done for the UCS test): 1) Because the high strain-rate response produces significant apparatus compliance, the specimen axial deformation, after being corrected for compliance, no longer follows an idealized linear ramp-and-hold response; as a result, the function  $\bar{\epsilon}(s)$  in Eq. (A1) does not have the simple form given in Eq. (A3) and its precise formulation is test-dependent. 2) The high strain-rate test requires sampling the response at very small times; small values of the time variable  $t$  correspond to large values of the Laplace transform variable  $s$ , resulting in longer computational times for the numerical Laplace inversion routine, which considerably slows down (and sometimes prevents completion of) the curve-fitting procedure. Both of these problems are completely alleviated by the use of the transient-to-harmonic transformation.

With regard to the hypothesis of this study, the experimental findings demonstrate that the biphasic-CLE-QLV model is indeed best able to describe the strain-rate-dependent mechanical response of articular cartilage in unconfined compression as attested by the high  $r^2$  values at slow and fast strain rates. Interestingly, the BPVE model also appears at first to produce encouraging results, with  $r^2$  values statistically different but only moderately smaller than for the biphasic-CLE-QLV model; the biphasic-CLE is clearly less successful in modeling both the UCS and UCF experiments simultaneously. Because of the similarity in the quality of curve-fits of the biphasic-CLE-QLV and the BPVE models, a closer scrutiny of the material properties derived from both models is necessary (Table 1). It is found that, in essence, the largest differences in material constants occur with the tensile modulus ( $H_{+A}$ ), and the intrinsic viscoelasticity parameters  $c$  and the ratio  $\tau_2/\tau_1$ . Physically, these differences can be explained as follows: In unconfined compression, a cartilage cylindrical plug is subjected to compression along its axial direction, and tension along its radial and circumferential (transverse) directions; given that cartilage exhibits different properties in tension and compression, as is copiously attested in the literature, rapid loading in unconfined compression will be resisted by very high tensile radial and hoop stresses, producing a much larger interstitial fluid pressurization, reaction force, and instantaneous modulus than could be predicted with a linear model alone [1,2,9,23,24,25,39]; if however the solid matrix also exhibits intrinsic viscoelasticity, the instantaneous modulus will be even higher because the rapid loading also produces further tissue stiffening. In the biphasic-CLE-QLV model, both of these effects are taken into account and are found to be significant, with  $H_{+A}$  significantly greater than  $H_{-A}$  and  $1 + c \ln \tau_2/\tau_1$  significantly greater than one. In the BPVE model, only the intrinsic viscoelasticity is modeled, since  $H_{+A} = H_{-A}$ ; consequently, in order to achieve a high peak response under rapid loading, higher values of the constant  $c$  or the ratio  $\tau_2/\tau_1$  are required as observed in this study. Indeed, according to theory, the instantaneous modulus in unconfined compression is given by  $E_{-Y}^{0+} = (1 + c \ln \tau_2/\tau_1)(H_{-A} - 3\lambda_2/2 + H_{+A}/2)$  for the biphasic-CLE-QLV model, which averages to 16.6 MPa for the properties in Table 1, and  $E_{-Y}^{0+} = 3(1 + c \ln \tau_2/\tau_1)(H_{-A} - \lambda_2)/2$  for the BPVE model, which averages to 20.1 MPa; both of these values are of the same order of magnitude, confirming that both models are able to predict a large and realistic instantaneous modulus in unconfined compression (Figs. 2 and 4). However, this study also showed that there was no agreement between the confined compression stress-relaxation results and the predictions of the BPVE model, when using  $c$ ,  $\tau_1$  and  $\tau_2$  as determined from unconfined compression tests. Since the cartilage response in confined compression is independent of tension-compression nonlin-

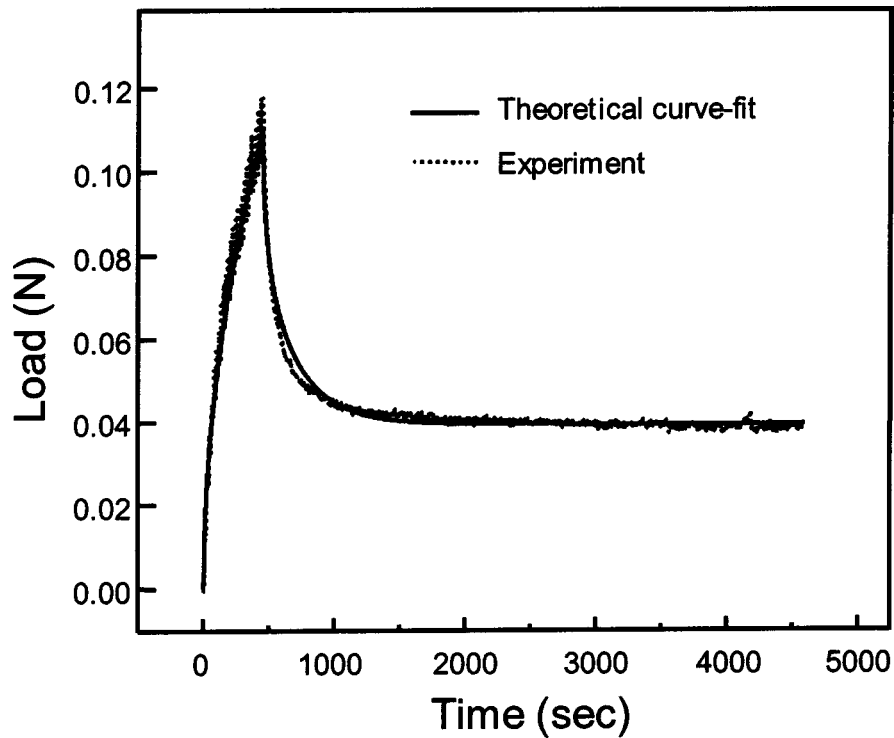


Fig. 5 Typical confined compression stress-relaxation (CCS) experimental response and theoretical curve-fit using the biphasic-CLE-QLV model

earity, the BPVE model may indeed have overestimated the QLV parameters during the curve-fitting of the experimental results in unconfined compression.

From our perspective, another limitation of the BPVE model, as with other constitutive models that assume the same modulus in tension and compression, is the inability to predict the transient and equilibrium tensile response of the tissue as well as the significant fluid pressurization in unconfined compression. As was shown in our recent study of the biphasic-CLE model [2], the tension-compression nonlinearity of cartilage acts to enhance interstitial fluid load support in unconfined compression by producing fluid pressures in very good agreement with experimental

measurements and far in excess of what may be predicted by constitutive models which employ the same modulus in tension and compression. Furthermore, our recent theoretical study of the biphasic-CLE-QLV model demonstrated that incorporation of solid matrix intrinsic viscoelasticity and tension-compression nonlinearity in the biphasic model improved the prediction of the cartilage responses to dynamic unconfined compression as well as uniaxial tension. These observations are illustrated by a representative uniaxial tensile test on a bovine cartilage strip harvested from one of the same joints used in the compression tests reported above, as shown in Fig. 7a, where a strain of 2.5% is applied over a ramp time of 208s. Theoretical predictions of a uniaxial tensile

Table 1 Mean and standard deviation of material properties for the biphasic-CLE-QLV, biphasic-CLE, and biphasic poroviscoelastic models (12 specimens).

Material Properties	Biphasic-CLE-QLV	Biphasic Poroviscoelastic	Biphasic-CLE	Biphasic-CLE (UCS only)
$H_{-A}$ (MPa)	$0.51 \pm 0.18^\dagger$	$0.51 \pm 0.18^\dagger$	$0.51 \pm 0.18^\dagger$	$0.51 \pm 0.18^\dagger$
$H_{+A}$ (MPa)	$8.8 \pm 2.5$	$(0.51 \pm 0.18)^\dagger$	$30.0 \pm 9.8$	$11.0 \pm 4.0$
$\lambda_2$ (MPa)	$0.30 \pm 0.13$	$0.20 \pm 0.09$	$0.36 \pm 0.21$	$0.34 \pm 0.21$
$k_r$ ( $m^4/N.s$ )	$1.07 \pm 0.46 \times 10^{-15}$	$0.74 \pm 0.54 \times 10^{-15}$	$2.76 \pm 0.57 \times 10^{-15}$	$0.98 \pm 0.29 \times 10^{-15}$
$c$	$0.51 \pm 0.23$	$5.98 \pm 2.31$	$(0)^\dagger$	$(0)^\dagger$
$\tau_1$ (s)	$0.77 \pm 0.54$	$0.38 \pm 0.39$		
$\tau_2$ (s)	$162 \pm 90$	$448 \pm 327$		
$k_z$ ( $m^4/N.s$ )	$1.44 \pm 0.89 \times 10^{-15}$	no convergence	$1.32 \pm 1.00 \times 10^{-15}$	$1.32 \pm 1.00 \times 10^{-15}$

<sup>†</sup>All theories share the same value of  $H_{-A}$ . In the biphasic poroviscoelastic theory,  $H_{+A} = H_{-A}$ ; in the biphasic-CLE theory,  $c=0$  and  $\tau_1, \tau_2$  are not defined.

Table 2 Mean and standard deviation of the coefficients of determination,  $r^2$ , for theoretical curve-fits of experimental data from UCS, UCF and CCS tests, for the biphasic-CLE-QLV, biphasic-CLE, and biphasic poroviscoelastic models (12 specimens).

Test	Biphasic-CLE-QLV	Biphasic Poroviscoelastic	Biphasic-CLE	Biphasic-CLE (UCS only)
UCS	$0.966 \pm 0.032$	$0.864 \pm 0.106$	$0.450 \pm 0.208$	$0.964 \pm 0.028$
UCF	$0.998 \pm 0.002$	$0.929 \pm 0.079$	$0.871 \pm 0.115$	
CCS	$0.951 \pm 0.035$	no convergence	$0.918 \pm 0.046$	$0.918 \pm 0.046$

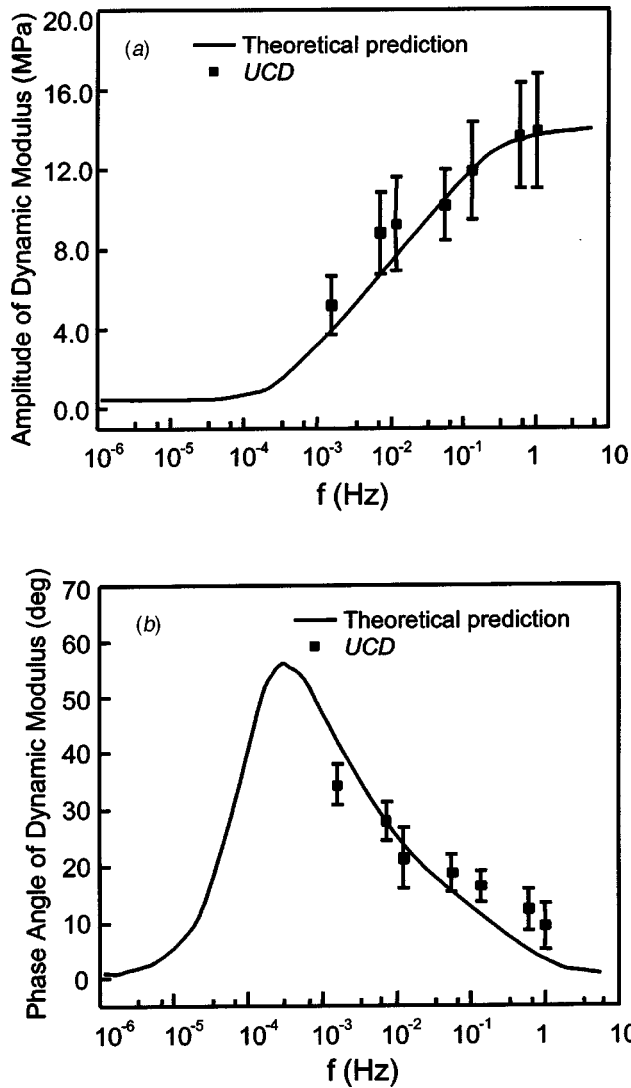


Fig. 6 Average results of (a) amplitude and (b) phase angle of the dynamic modulus as measured from the *UCD* test, together with the theoretical prediction from the biphasic-CLE-QLV model using the mean values of the material properties curve-fitted from the *CCS*, *UCS* and *UCF* tests (6 specimens)

test under the same loading conditions are shown for the biphasic-CLE-QLV and the BPVE models in Fig. 7b using the average properties listed in Table 1. The observed difference in the order of magnitude of the responses indicates that only the biphasic-CLE-QLV model shows more consistency with the experimental tensile response over the given time period (2000 sec). Similarly, a representative experimental interstitial fluid pressure response reported in our earlier study [2] is shown in Fig. 8a. In that earlier study, an unconfined compression stress-relaxation test was performed on cylindrical bovine articular cartilage plugs (diam. 4.78 mm), where a strain of 10% was applied over a ramp time of 280s and a peak fluid pressure of 0.42 MPa was measured at the center of the articular surface (over a circular footprint, 1 mm in diameter). Theoretical predictions from the biphasic-CLE-QLV and the BPVE models, using the average properties in Table 1, are shown in Fig. 8b, similarly demonstrating that the BPVE model is unable to predict the high values of interstitial fluid pressure in this testing configuration.

Interestingly, though fitting the biphasic-CLE model to both *UCS* and *UCF* data produces unsatisfactory results (Table 2), the *UCS* data alone can be very well curve-fitted with this model [2]

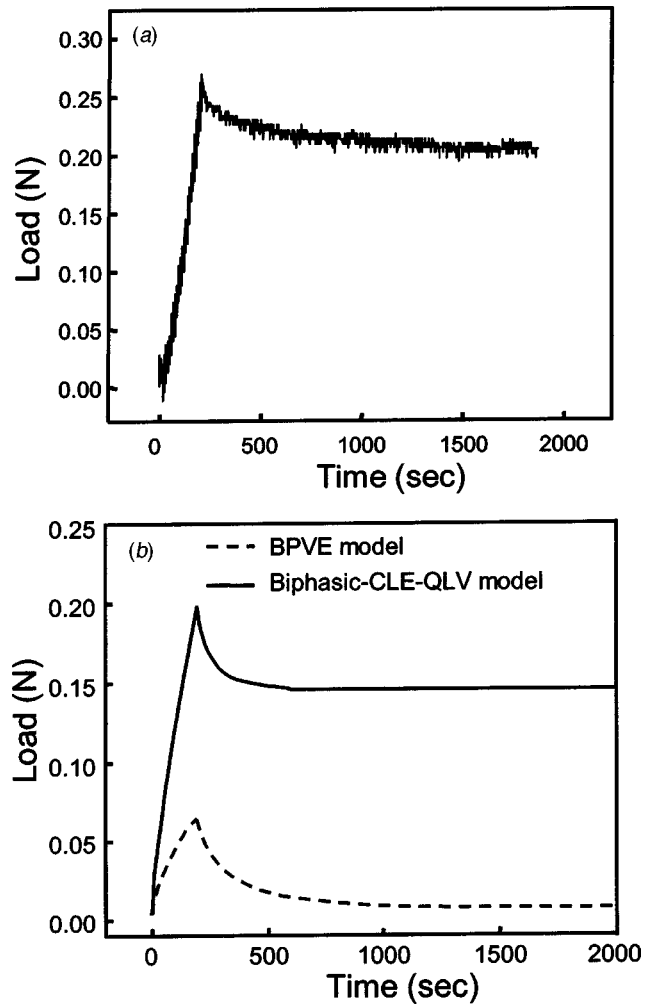
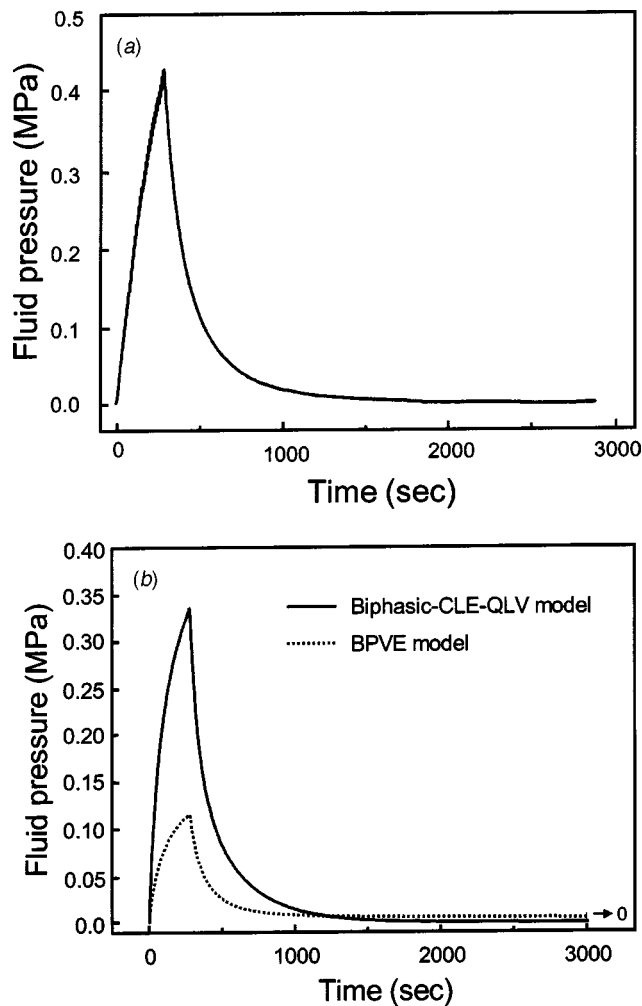


Fig. 7 (a) A representative experimental response in uniaxial tension from a single sample of bovine cartilage. (b) Theoretical responses of biphasic-CLE-QLV and BPVE models in uniaxial tension using the average properties listed in Table 1.

producing elastic constants and permeabilities which are not statistically different from their corresponding values from the biphasic-CLE-QLV model. According to Table 1,  $H_{+A}$  is overestimated by 25% and  $\lambda_2$  by 13% on average when using the biphasic-CLE model with the strain rates employed in this study for the *UCS* tests. Based on our understanding of the underlying mechanisms governing the tissue response, we estimate that slower strain rates may produce even better agreement in the values of  $H_{+A}$ ,  $\lambda_2$  and  $k_r$  between the biphasic-CLE-QLV and the biphasic-CLE models. This suggests that unconfined compression experiments with a sufficiently slow ramp, as performed in our earlier study [2], can produce reasonable estimates of a subset of the material properties required to completely characterize the compressive behavior of the tissue. However, to model the response of cartilage at higher loading frequencies, additional tests would be required to acquire the intrinsic viscoelasticity properties as well (such as the *UCF* test employed here, or uniaxial tensile tests).

It may seem at first that employing a constitutive relation with eight material parameters is bound to produce good agreement between theory and experiments, and that the successful outcome of the current study was a foregone conclusion. It should be noted in this respect that because of the large number of parameters, a correspondingly large number of tests (*CCS*, *UCS*, *UCF*, *UCD*) was conducted on the same specimen samples, averaging two pa-



**Fig. 8** (a) A representative experimental response of interstitial fluid pressure reported in our earlier study [2] for unconfined compression stress-relaxation test on cylindrical bovine articular cartilage plugs (diam. 4.78 mm). Pressure was measured at the center of the articular surface, over a circular footprint 1 mm in diameter. (b) Theoretical predictions of interstitial fluid pressure response responses in unconfined compression stress-relaxation test from the biphasic-CLE-QLV and BPVE models using the average properties listed in Table 1. The BPVE model is unable to predict the elevated fluid pressures observed experimentally.

rameters per test. To our knowledge, this represents one of the more extensive series of tests, performed on the same samples of cartilage, reported in the literature. Based on theory [34], the experimental response of each test is mainly governed by a subset of material parameters. The equilibrium state of the *CCS* test is determined by  $H_{-A}$  only. Given  $H_{-A}$  from the *CCS* test, the equilibrium state (equilibrium Young's modulus, i.e., Eq. (A5) of the *UCS* test is only dependent on  $H_{+A}$  and  $\lambda_2$ , while the stress-relaxation phase of the *UCS* test is also dependent on  $k_r$ . Given the elastic constants, the dynamic response of cartilage at high strain rate (*UCF* test) is primarily governed by the QLV parameters ( $c$ ,  $\tau_1$  and  $\tau_2$ ). After obtaining  $H_{-A}$ ,  $c$ ,  $\tau_1$  and  $\tau_2$ , the transient response of *CCS* is governed by  $k_z$  only. Finally, given all the material constants curve-fitted from the *CCS*, *UCS* and *UCF* tests, the experimental data of the *UCD* test was predicted successfully from the theory (Fig. 6). The strategy employed in this study for determining the eight material parameters of the theory from multiple tests may explain why our results are consistent with those reported in previous studies [2,22]. Neverthe-

less, some of the material parameters could be individually measured through more direct testing configurations. For example,  $H_{+A}$  could be determined from the equilibrium state of an axial tensile test while  $\lambda_2$  could be determined from the equilibrium ratio of radial stress to axial strain in confined compression [36]. Similarly, permeation experiments could be used to determine the permeabilities more directly. Therefore, the parameters obtained in this study may need to be verified by more direct measurements. However, it should be noted that such alternative testing configurations may require specimen geometries and orientation which are incompatible among all the necessary tests, whereas the tests conducted in the current study could all be performed on the same cylindrical specimen plug harvested perpendicular to the articular surface.

In summary, this experimental study provides strong evidence for the hypothesis that both tension-compression nonlinearity and intrinsic viscoelasticity of the solid matrix of cartilage are necessary for modeling the transient and equilibrium responses of this tissue in tension and compression. This hypothesis was tested by curve-fitting experimental data to a biphasic-CLE-QLV model, and simpler models subsumed by this more general framework. Whether the precise constitutive formulation employed here is optimal for articular cartilage remains to be verified against additional experimental data, e.g., including uniaxial tensile, shear, and torsion tests. For example, the assumption that the equilibrium response of cartilage is piecewise linear (linear in tension and linear in compression, though with different slopes), is a simplification of the real behavior of cartilage. The assumption of linear viscoelasticity may also prove to be a simplification, though the good agreement found in this study between the experimental time domain and frequency domain responses, as attested by the linear Laplace transform methodology [38], suggests that the linear viscoelasticity assumption may indeed be appropriate. The findings of this study help explain why seemingly competing theories described in the literature, such as the BPVE, the biphasic-CLE, and other similar models, have been successful at predicting various unconfined compression experiments while employing different modeling assumptions regarding the solid matrix of the tissue. A more comprehensive model seems to require the incorporation of all of these previous modeling assumptions, including the porous-permeable biphasic nature, the tension-compression nonlinearity and the intrinsic viscoelasticity of the solid matrix.

Finally, the peak dynamic unconfined compression modulus measured from the *UCD* tests averages 14 MPa at the frequency of 1 Hz (Fig. 6); this result is comparable with previous studies reporting a range of 12–20 MPa [25,26,39]. It explains how articular cartilage can routinely sustain physiological stress levels from 3 to 6 MPa while its collagen-proteoglycan matrix exhibits a compressive modulus as low as 0.51 MPa as was observed in this study. Thus, intrinsic viscoelasticity and tension-compression nonlinearity of articular cartilage do play important roles in the load-support mechanism of cartilage under physiologic loading.

### Acknowledgments

This study was supported with funds from the National Institute of Arthritis and Musculoskeletal and Skin Diseases of the National Institutes of Health (AR46532, AR43628, AR41918).

### Appendix A: Biphasic-CLE-QLV Model

**Unconfined Compression.** The reduction of the general biphasic equations to the configuration of unconfined compression with frictionless platens and axisymmetric conditions has been described previously for the linear isotropic biphasic model [23], the biphasic poroviscoelastic model [40], and the biphasic-CLE model [2]. As is typical for this type of problems, the closed-form solution for the biphasic-CLE-QLV model is given in Laplace transform space [34]:

$$\frac{\bar{F}(s)}{\pi r_0^2} = H_{+A} \left( 1 + c \ln \frac{1 + \tau_2 s}{1 + \tau_1 s} \right) \left\{ \frac{\left( \frac{2H_{-A} - 3\lambda_2 + H_{+A}}{2H_{+A}} \right) \sqrt{f} I_0(\sqrt{f}) + \left( 1 - \frac{\lambda_2}{H_{+A}} \right) \left( \frac{2\lambda_2 - H_{-A} - H_{+A}}{H_{+A}} \right) I_1(\sqrt{f})}{\sqrt{f} I_0(\sqrt{f}) - \left( 1 - \frac{\lambda_2}{H_{+A}} \right) I_1(\sqrt{f})} \right\} \bar{\varepsilon}(s), \quad (A1)$$

where

$$f = \frac{r_0^2 s}{H_{+A} k_r \left( 1 + c \ln \frac{1 + \tau_2 s}{1 + \tau_1 s} \right)}. \quad (A2)$$

In these equations,  $\varepsilon$  is the axial strain,  $F$  is the total axial force across the specimen,  $r_0$  is the specimen radius,  $\lambda_2$  is the “off-diagonal” modulus,  $k_r$  is the radial permeability, and  $c$ ,  $\tau_1$  and  $\tau_2$  are the QLV parameters).  $I_0(\cdot)$  and  $I_1(\cdot)$  are modified Bessel functions of the first kind, of order 0 and 1, respectively. Overbars indicate Laplace transformation from the time domain and  $s$  is the Laplace transform variable. The aggregate moduli in tension and compression are given by  $H_{+A}$  and  $H_{-A}$ .

These solutions are valid for a variety of loading conditions. If the strain is ramped over a ramp time of  $t_0$  and subsequently kept constant at a magnitude of  $\varepsilon_0$ , use

$$\bar{\varepsilon}(s) = -(1 - e^{-st_0}) \varepsilon_0 / s^2 t_0. \quad (A3)$$

Then, inverse Laplace transformation into the time domain can be performed numerically, using the INLAP routine from the IMSL library (Visual Numerics Inc., Houston, TX). For the steady-state solution to a sinusoidal axial load or strain, it suffices to substitute  $s = j\omega$  into the solutions of Eqs. (A1)–(A2), where  $\omega$  is the angular frequency of the applied load or strain and  $j = \sqrt{-1}$ , to derive the frequency-dependent amplitude and phase response of the corresponding parameter. The dynamic modulus  $\bar{G}(s)$  of this biphasic-CLE-QLV material can be derived from the ratio of  $\bar{F}(s)/\pi r_0^2$  and  $\bar{\varepsilon}(s)$  in Eq. (A1). To determine the material’s “instantaneous” unconfined compression modulus (or the unconfined compression modulus in the limit of loading at high frequency), denoted by  $E_{-y}^+$ , it suffices to take the limit of the resulting expression as  $s \rightarrow \infty$  which corresponds to the real time limit of  $t \rightarrow 0^+$ :

$$E_{-y}^+ = \left( 1 + c \ln \frac{\tau_2}{\tau_1} \right) \left( H_{-A} - \frac{3}{2} \lambda_2 + \frac{H_{+A}}{2} \right). \quad (A4)$$

Similarly, the unconfined compression modulus at equilibrium (or in the limit of loading at very low frequency),  $E_{-y}$ , can be obtained by taking the limit of the dynamic modulus as  $s \rightarrow 0$ ,

$$E_{-y} = H_{-A} - \frac{2\lambda_2^2}{H_{+A} + \lambda_2}. \quad (A5)$$

## Appendix B: Conversion of Experimental Response From Time Domain to Frequency Domain

In recent publications, Buschmann and co-workers [38,39] proposed a methodology for converting creep or stress-relaxation data from the time domain into the frequency domain, thereby extracting the steady-state frequency response of the dynamic modulus from a transient experiment. This methodology was adapted in the current study as follows: Experimental measurements of the axial displacement  $u(t)$  and reaction force  $F(t)$  were acquired at discrete time increments  $t_i$ , in the range  $0 \leq t_i \leq t_{eq}$  where equilibrium conditions prevailed at the last time step  $t_{eq}$ ; the axial strain was calculated from  $\varepsilon(t_i) = u(t_i)/h \equiv \varepsilon_i$  whereas the axial stress was calculated from  $\sigma(t_i) = F(t_i)/\pi r_0^2 \equiv \sigma_i$ . Linear interpolation was assumed between two consecutive time steps,  $t_i$  and  $t_{i+1}$ , e.g., for the strain,

$$\varepsilon(t) = \varepsilon_i + \frac{t - t_i}{t_{i+1} - t_i} (\varepsilon_{i+1} - \varepsilon_i) [H(t - t_i) - H(t - t_{i+1})] \text{ when } t_i \leq t < t_{i+1}, \quad (B1)$$

where  $H(t)$  is the Heaviside step function. The general Laplace transform of this equation is

$$\bar{\varepsilon}(s) = \frac{\varepsilon_{i+1} - \varepsilon_i}{s^2(t_{i+1} - t_i)} (e^{-st_i} - e^{-st_{i+1}}) + \frac{\varepsilon_i e^{-st_i}}{s} - \frac{\varepsilon_{i+1} e^{-st_{i+1}}}{s} \text{ when } t_i \leq t < t_{i+1}. \quad (B2)$$

For  $t \geq t_{eq}$ , the axial strain can be taken to behave as  $\varepsilon(t) = \varepsilon_{eq} H(t - t_{eq})$ , whose Laplace transform is  $\bar{\varepsilon}(s) = \varepsilon_{eq} e^{-st_{eq}}/s$ , whereas for  $t=0$  it can be assumed that  $\varepsilon(0)=0$ . Combining these results with those of Eq. (B2) by taking a summation over all time steps produces a function valid for  $0 \leq t < \infty$ ,

$$\bar{\varepsilon}(s) = \sum_{i=1}^{n-1} \frac{\varepsilon_{i+1} - \varepsilon_i}{s^2(t_{i+1} - t_i)} (e^{-st_i} - e^{-st_{i+1}}), \quad (B3)$$

where  $n$  is the number of time increments. By an identical process,

$$\bar{\sigma}(s) = \sum_{i=1}^{n-1} \frac{\sigma_{i+1} - \sigma_i}{s^2(t_{i+1} - t_i)} (e^{-st_i} - e^{-st_{i+1}}), \quad (B4)$$

and thus the dynamic modulus is given by

$$\bar{G}(s) = \frac{\sum_{i=1}^{n-1} \frac{\sigma_{i+1} - \sigma_i}{(t_{i+1} - t_i)} (e^{-st_i} - e^{-st_{i+1}})}{\sum_{i=1}^{n-1} \frac{\varepsilon_{i+1} - \varepsilon_i}{(t_{i+1} - t_i)} (e^{-st_i} - e^{-st_{i+1}})}. \quad (B5)$$

This complex function can be evaluated for any desired  $s = j\omega$  to provide the steady-state frequency response of the dynamic modulus. In practice, depending on the frequency content of the experimental data, there exists an upper bound on  $\omega$  above which this evaluation produces invalid results. For a stress-relaxation test with a ramp time of  $t_0$ , a rule of thumb may be that the frequency content cannot be greater than  $1/t_0$  ( $\omega < 2\pi/t_0$ ); for the UCF tests of the current study, an upper bound of 3 Hz was employed for all specimens.

## References

- [1] Souhat, J., Buschmann, M. D., and Shirazi-Adl, A., 1999, “A Fibril-Network Reinforced Model of Cartilage in Unconfined Compression,” *J. Biomech. Eng.*, **121**, pp. 340–347.
- [2] Soltz, M. A., and Ateshian, G. A., 2000, “A Conewise Linear Elasticity Mixture Model for the Analysis of Tension-Compression Nonlinearity in Articular Cartilage,” *J. Biomech. Eng.*, **122**, pp. 576–586.
- [3] Mow, V. C., Kuei, S. C., Lai, W. M., and Armstrong, C. G., 1980, “Biphasic Creep and Stress Relaxation of Articular Cartilage in Compression: Theory and Experiments,” *J. Biomech. Eng.*, **102**, pp. 73–84.
- [4] Mak, A. F., 1986, “The Apparent Viscoelastic Behavior of Articular Cartilage—The Contributions from the Intrinsic Matrix Viscoelasticity and Interstitial Fluid Flows,” *J. Biomech. Eng.*, **108**, pp. 123–130.
- [5] DiSilvestro, M. R., Zhu, Q., and Suh, J.-K., 1999, “Biphasic Poroviscoelastic Theory Predicts the Strain Rate Dependent Viscoelastic Behavior of Articular Cartilage,” *Proc. 1999 Bioeng. Conf., ASME BED-42*, pp. 105–106.
- [6] Holmes, M. H., Lai, W. M., and Mow, V. C., 1985, “Singular Perturbation Analysis of the Nonlinear, Flow-Dependent Compressive Stress Relaxation Behavior of Articular Cartilage,” *J. Biomech. Eng.*, **107**, pp. 206–218.

- [7] Kwan, M. K., Lai, W. M., and Mow, V. C., 1990, "A Finite Deformation Theory for Cartilage and Other Soft Hydrated Connective Tissues—I. Equilibrium Results," *J. Biomech.*, **23**, pp. 145–155.
- [8] Holmes, M. H., and Mow, V. C., 1990, "The Nonlinear Characteristics of Soft Eels and Hydrated Connective Tissues in Ultrafiltration," *J. Biomech.*, **23**, pp. 1145–1156.
- [9] Cohen, B., Lai, W. M., and Mow, V. C., 1998, "A Transversely Isotropic Biphasic Model for Unconfined Compression of Growth Plate and Chondroepiphysis," *J. Biomech. Eng.*, **120**, pp. 491–496.
- [10] Fung, Y.-C. B., 1972, "Stress-Strain History Relation of Soft Tissues in Simple Elongation," In *Biomechanics: Its Foundations and Objectives*, Prentice Hall, Englewood Cliffs, 1972.
- [11] Frank, E. H., and Grodzinsky, A. J., 1987, "Cartilage Electromechanics—II. A Continuum Model of Cartilage Electrokinetics and Correlation with Experiments," *J. Biomech.*, **20**, pp. 629–639.
- [12] Lai, W. M., Hou, J. S., and Mow, V. C., 1991, "A Triphasic Theory for the Swelling and Deformation Behaviors of Articular Cartilage," *J. Biomech. Eng.*, **113**, pp. 245–258.
- [13] Gu, W. Y., Lai, W. M., and Mow, V. C., 1998, "A Mixture Theory for Charged Hydrated Soft Tissues Containing Multi-electrolytes: Passive Transport and Swelling Behaviors," *J. Biomech. Eng.*, **102**, pp. 169–180.
- [14] Huyghe, J. M., and Janssen, J. D., 1997, "Quadruphase Mechanics of Swelling Incompressible Porous Media," *Int. J. Eng. Sci.*, **35**, pp. 793–802.
- [15] Farquhar, T., Dawson, P. R., and Torzilli, P. A., 1990, "A Microstructural Model for the Anisotropic Drained Stiffness of Articular Cartilage," *J. Biomech. Eng.*, **112**, pp. 414–425.
- [16] Wren, T. A., and Carter, D. R., 1998, "A Microstructural Model for the Tensile Constitutive and Failure Behavior of Soft Skeletal Connective Tissues," *J. Biomech. Eng.*, **120**, pp. 55–61.
- [17] Bursac, P. M., McGrath, C. V., Eisenberg, S. R., and Stamenovic, D., 2000, "A Microstructural Model of Elastostatic Properties of Articular Cartilage in Confined Compression," *J. Biomech. Eng.*, **122**, pp. 347–353.
- [18] Ateshian, G. A., Warden, W. H., Kim, J. J., Grelsamer, R. P., and Mow, V. C., 1997, "Finite Deformation Biphasic Material Properties of Bovine Articular Cartilage from Confined Compression Experiments," *J. Biomech.*, **30**, pp. 1157–1164.
- [19] Soltz, M. A., and Ateshian, G. A., 1998, "Experimental Verification and Theoretical Prediction of Cartilage Interstitial Fluid Pressurization At An Impermeable Contact Interface in Confined Compression," *J. Biomech.*, **31**, pp. 927–994.
- [20] Soltz, M. A., and Ateshian, G. A., 2000, "Interstitial Fluid Pressurization During Confined Compression Cyclical Loading of Articular Cartilage," *Ann. Biomed. Eng.*, **28**, pp. 150–159.
- [21] Bursac, P. M., Obitz, T. W., Eisenberg, S. R., and Stamenovic, D., 1999, "Confined and Unconfined Stress Relaxation of Cartilage: Appropriateness of a Transversely Isotropic Analysis," *J. Biomech.*, **32**, pp. 1125–1130.
- [22] Setton, L. A., Zhu, W., and Mow, V. C., 1993, "The Biphasic Poroviscoelastic Behavior of Articular Cartilage: Role of the Surface Zone in Governing the Compressive Behavior," *J. Biomech.*, **26**, pp. 581–592.
- [23] Armstrong, C. G., Lai, W. M., and Mow, V. C., 1984, "An Analysis of Unconfined Compression of Articular Cartilage," *J. Biomech.*, **106**, pp. 165–173.
- [24] Brown, T. D., and Singerman, R. J., 1986, "Experimental Determination of the Linear Biphasic Constitutive Coefficients of Human Fetal Proximal Femoral Chondroepiphysis," *J. Biomech.*, **19**, pp. 597–605.
- [25] Kim, Y. J., Bonassar, L. J., and Grodzinsky, A. J., 1995, "The Role of Cartilage Streaming Potential, Fluid Flow and Pressure in the Stimulation of Chondrocyte Biosynthesis During Dynamic Compression," *J. Biomech.*, **28**, pp. 1055–1066.
- [26] Buschmann, M. D., Kim, Y. J., Wong, M., Frank, E., Hunziker, E. B., and Grodzinsky, A. J., 1999, "Stimulation of Aggrecan Synthesis in Cartilage Explants By Cyclic Loading Is Localized To Regions of High Interstitial Fluid Flow," *Arch. Biochem. Biophys.*, **366**, pp. 1–7.
- [27] Mak, A. F., Lai, W. M., and Mow, V. C., 1987, "Biphasic Indentation of Articular Cartilage—I. Theoretical Analysis," *J. Biomech.*, **20**, pp. 703–714.
- [28] Mow, V. C., Gibbs, M. C., Lai, W. M., Zhu, W., and Athanasiou, K. A., 1989, "Biphasic Indentation of Articular Cartilage-Part II. A Numerical Algorithm and an Experimental Study," *J. Biomech.*, **22**, pp. 853–861.
- [29] Athanasiou, K. A., Rosenwasser, M. P., Buckwalter, J. A., Malinin, T. I., and Mow, V. C., 1991, "Interspecies Comparisons of in situ Intrinsic Mechanical Properties of Distal Femoral Cartilage," *J. Orthop. Res.*, **9**, pp. 330–340.
- [30] Hale, J. E., Rudert, M. J., and Brown, T. D., 1993, "Indentation Assessment of Biphasic Mechanical Property Deficits in Size-Dependent Osteochondral Defect Repair," *J. Biomech.*, **26**, pp. 1319–1325.
- [31] Mow, V. C., Good, P. M., and Gardner, T. R., 2000, "A New Method To Determine the Tensile Properties of Articular Cartilage Using the Indentation Test," *Trans. Annu. Meet. — Orthop. Res. Soc.*, **25**, p. 103.
- [32] Suh, J. K., and Bai, S., 1997, "Biphasic Poroviscoelastic Behavior of Articular Cartilage in Creep Indentation Test," *Trans. Annu. Meet. — Orthop. Res. Soc.*, **22**, p. 823.
- [33] Woo, S. L.-Y., Simon, B. R., Kuei, S. C., and Akeson, W. H., 1980, "Quasi-Linear Viscoelastic Properties of Normal Articular Cartilage," *J. Biomech. Eng.*, **102**, pp. 85–90.
- [34] Huang, C.-Y., Mow, V. C., and Ateshian, G. A., 2001, "The Role of Flow-independent Viscoelasticity In The Tensile Response of Biphasic Articular Cartilage," *J. Biomech. Eng.*, **123**, pp. 410–417.
- [35] Curnier, A., He, Q.-C., and Zysset, P., 1995, "Conewise Linear Elastic Materials," *J. Elast.*, **37**, pp. 1–38.
- [36] Khalsa, P. S., and Eisenberg, S. R., 1997, "Compressive Behavior of Articular Cartilage Is Not Completely Explained by Proteoglycan Osmotic Pressure," *J. Biomech.*, **30**, pp. 589–594.
- [37] Kvalseth, T. O., 1985, "Cautionary Note About  $R^2$ ," *Am. Stat.*, **39**, pp. 279–285.
- [38] Buschmann, M. D., 1997, "Numerical Conversion of Transient to Harmonic Response Functions for Linear Viscoelastic Materials," *J. Biomech.*, **30**, pp. 197–202.
- [39] Fortin, M., Soulhat, J., Shirazi-Adl, A., Hunziker, E. B., and Buschmann, M. D., 2000, "Unconfined Compression of Articular Cartilage: Nonlinear Behavior and Comparison with a Fibril-Reinforced Biphasic Model," *J. Biomech. Eng.*, **122**, pp. 189–195.
- [40] Mak, A. F., 1986, "Unconfined Compression of Hydrated Viscoelastic Tissues: A Biphasic Poroviscoelastic Analysis," *Biorheology*, **23**, pp. 371–383.